Volume 354, Number 1, 18 November 2005 ISSN 0022-2836

ELSEVIER

JMB

JOURNAL OF MOLECULAR BIOLOGY

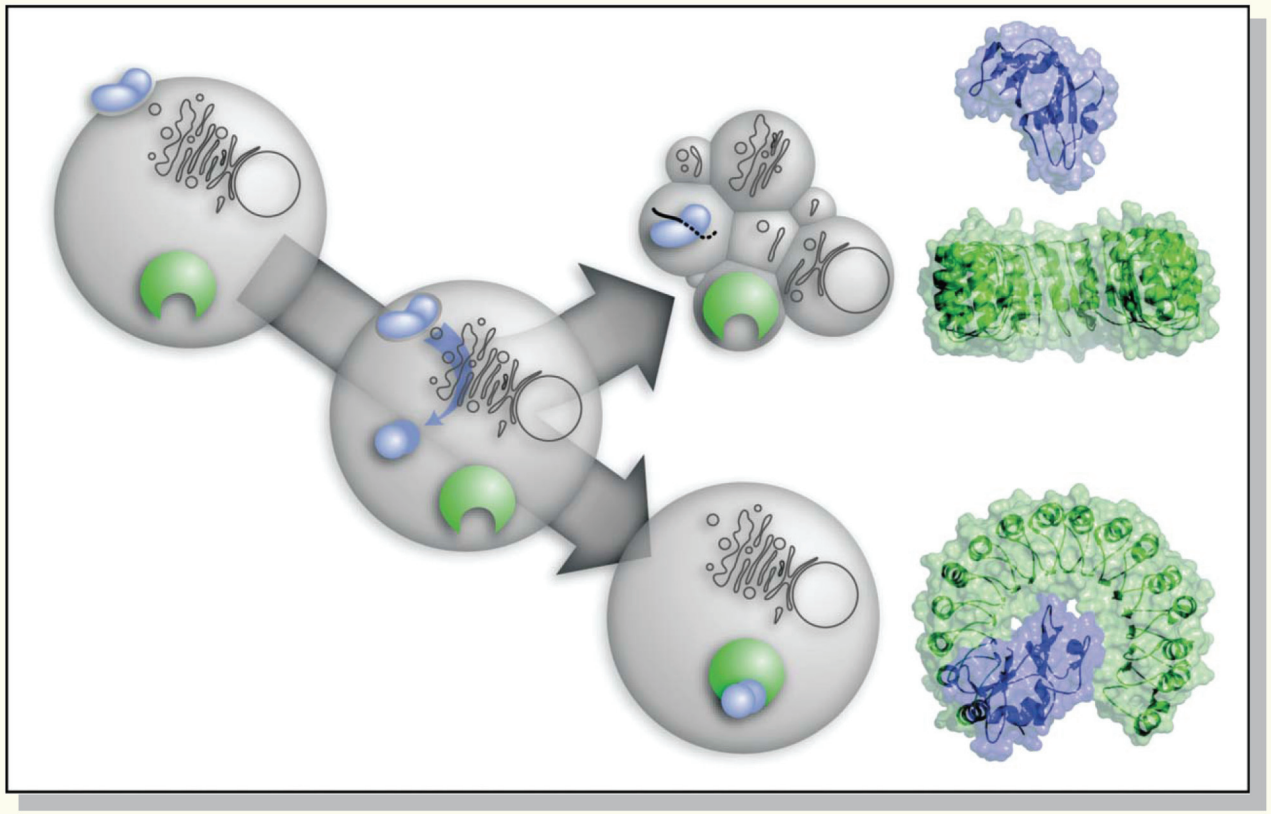

doi:10.1016/j.jmb.2005.08.007 J. Mol. Biol. (2005) 354, 41–54

JMB

Available online at www.sciencedirect.com

SCIENCE DIRECT®

ELSEVIER

Disruption of Shape-Complementarity Markers to Create Cytotoxic Variants of Ribonuclease A

Thomas J. Rutkoski[1], Erin L. Kurten[1], Julie C. Mitchell[1,2]* and Ronald T. Raines[1,3]*

[1]*Department of Biochemistry University of Wisconsin-Madison, Madison, WI 53706, USA*

[2]*Department of Mathematics University of Wisconsin-Madison, Madison, WI 53706, USA*

[3]*Department of Chemistry University of Wisconsin-Madison, Madison, WI 53706, USA*

**Corresponding author*

Onconase® (ONC), an amphibian member of the bovine pancreatic ribonuclease A (RNase A) superfamily, is in phase III clinical trials as a treatment for malignant mesothelioma. RNase A is a far more efficient catalyst of RNA cleavage than ONC but is not cytotoxic. The innate ability of ONC to evade the cytosolic ribonuclease inhibitor protein (RI) is likely to be a primary reason for its cytotoxicity. In contrast, the non-covalent interaction between RNase A and RI is one of the strongest known, with the RI·RNase A complex having a K_d value in the femtomolar range. Here, we report on the use of the fast atomic density evaluation (FADE) algorithm to identify regions in the molecular interface of the RI·RNase A complex that exhibit a high degree of geometric complementarity. Guided by these "knobs" and "holes", we designed variants of RNase A that evade RI. The D38R/R39D/N67R/G88R substitution increased the K_d value of the pRI·RNase A complex by 20×10^6-fold (to 1.4 μM) with little change to catalytic activity or conformational stability. This and two related variants of RNase A were more toxic to human cancer cells than was ONC. Notably, these cytotoxic variants exerted their toxic activity on cancer cells selectively, and more selectively than did ONC. Substitutions that further diminish affinity for RI (which has a cytosolic concentration of 4 μM) are unlikely to produce a substantial increase in cytotoxic activity. These results demonstrate the utility of the FADE algorithm in the examination of protein–protein interfaces and represent a landmark towards the goal of developing chemotherapeutics based on mammalian ribonucleases.

Keywords: cancer; cytotoxin; ribonuclease inhibitor; Onconase®; protein–protein interaction

Introduction

Bovine pancreatic ribonuclease (RNase A) catalyzes the cleavage of RNA.[1] Its putative biological function is to break down the large amounts of RNA that accumulate in the ruminant gut. Other members of the RNase A superfamily possess a variety of interesting biological properties, including antiproliferative, cytotoxic, embryotoxic, aspermatogenic, and antitumoral activities.[2–5] Originally isolated from oocytes and early embryos of the Northern leopard frog *Rana pipiens*,[6,7] Onconase® (ONC) is an amphibian homolog of RNase A that exhibits anti-tumoral activity both *in vitro* and *in vivo*.[8] The ability of ONC to hydrolyze RNA is essential to its cytotoxicity.[9] ONC is currently being evaluated as a treatment for malignant mesothelioma in phase III clinical trials.[10]

A significant practical limitation on the use of ONC as a chemotherapeutic is its dose-limiting renal toxicity.[11] Pharmacokinetic and biodistribution studies have revealed the renal retention of ONC to be 50–100-fold greater than that of

Abbreviations used: BS-RNase, bovine seminal ribonuclease; FADE, fast atomic density evaluation; 6-FAM, 6-carboxyfluorescein; hRI, human ribonuclease inhibitor; MALDI-TOF, matrix-assisted laser desorption/ionization time-of-flight; ONC, Onconase®; PBS, phosphate-buffered saline; PDB, protein data bank; pRI, porcine ribonuclease inhibitor; RI, ribonuclease inhibitor; RNase A, bovine pancreatic ribonuclease A; 6-TAMRA, 6-carboxytetramethylrhodamine; TB, Terrific Broth; TI, therapeutic index.

E-mail addresses of the corresponding authors: mitchell@math.wisc.edu; raines@biochem.wisc.edu

mammalian members of the RNase A superfamily.[12,13] Additionally, mice produce neutralizing antibodies against ONC but not against RNase A.[14] ONC shares only 30% amino acid sequence identity with RNase A.[15] Development of cytotoxic mammalian ribonucleases could thus provide a more appealing class of cancer therapeutics due to more favorable tissue distribution and reduced propensity for eliciting an immune response.[3]

Ribonuclease inhibitor (RI) is a 50 kDa protein found in the cytosol of all mammalian cells.[16–18] RI is a member of the leucine-rich repeat family of proteins and is composed of 15 alternating repeats arranged symmetrically to define a horseshoe shape.[19] Having 30 (porcine) or 32 (human) reduced cysteine residues,[20] RI can function only in a reducing environment like that of the cytosol.[21] There, RI acts as a sentry against invading ribonucleases,[22] binding to members of the RNase A superfamily in a 1:1 stoichiometry,[23] and inhibiting completely their catalytic activity by steric occlusion of the active site.[24] The complexes formed between RI and its ligands are among the tightest of known biomolecular associations, with equilibrium dissociation constants in the femtomolar range.[25]

Some RNase A superfamily members, such as ONC and bovine seminal ribonuclease (BS-RNase), possess the ability to evade RI. Evasion is achieved either by virtue of a unique quaternary structure, as in dimeric BS-RNase,[26,27] or by divergent tertiary structure, as in ONC,[9] which has severe truncations in its surface loops.[12] The ability to retain ribonucleolytic activity in the presence of RI is a primary determinant of the cytotoxicity of ONC and BS-RNase. We had shown that altering RNase A so as to destabilize the RI·RNase A complex can endow RNase A with cytotoxic activity.[28] Still, the most cytotoxic variant to date, K7A/G88R RNase A, has nanomolar affinity for porcine RI (pRI) and is nearly tenfold less cytotoxic than ONC.[29] Although the affinity of the K7A/G88R variant for RI is 10^5-fold less than that of wild-type RNase A, its affinity still greatly exceeds that of ONC (estimated $K_d \geq 10^{-6}$ M).[12]

Here, we implement a powerful computational tool to guide the design of new RI-evasive variants of RNase A. Specifically, we use the fast atomic density evaluation (FADE) algorithm[30] to identify the "knobs" and "holes" in the molecular interface of the pRI·RNase A complex.[31] The FADE algorithm approximates the shape of macromolecules by calculating the atomic density at points near the molecular surface. A counting algorithm is used to sum the atomic neighbors as a function of increasing radius from each discrete point. Intuitively, a surface region within a crevice is surrounded by atoms, and so would be expected to have a greater number of atomic neighbors (high atomic density) than would a surface region near a protrusion (low atomic density). To obtain a measure of local shape complementarity for a molecular complex, a three-dimensional grid of points is modeled onto the interface. The atomic density at each point on the grid is calculated with respect to each molecular component comprising the interface and the degree to which the "knobs" of one surface correspond with the "holes" on another is quantified. The descriptor of shape complementarity generated by FADE assigns the greatest significance to regions of the interface possessing adjacent surfaces with the most disparate atomic densities. In several model protein complexes, regions of high shape complementarity identified by FADE were shown to correlate well with amino acid residues identified in mutational studies as being important for binding affinity.[32] We reasoned that introducing electrostatic and steric incompatibilities in these regions would destabilize the pRI·RNase A complex. We describe the specific amino acid substitutions made to RNase A, the impact of these substitutions on RI affinity as well as catalytic activity and conformational stability, and how this approach ultimately resulted in several RNase A variants that are more toxic than ONC to tumor cells *in vitro*.

Results

FADE analysis

The results of the FADE analysis on the pRI·RNase A complex (PDB entry 1DFJ)[33] are depicted in Figures 1 and 2, where FADE geometric-complementarity markers are displayed as solid spheres. These spheres do not represent atoms. Instead, the spheres represent points in the molecular interface near which local complementarity is most significant. Complementarity markers within 2 Å of any atom within a particular residue were summed to determine the cluster sizes given in Table 1. The residues in RNase A that are proximal to the largest number of complementarity markers and distal from the enzymic active site[34] were targeted for disruption. We refrained from changing residues in RI because a goal of our work was to develop new cytotoxic ribonucleases.

We reasoned that disruption could, in general, be achieved best by replacing small neutral or anionic residues in RNase A with arginine. We suspected that arginine, as the most polar and second largest amino acid,[35] could generate electrostatic repulsion and steric strain while increasing the net positive charge, which is known to enhance cell internalization.[36] In addition, we replaced lysine residues in RNase A with alanine to create truncated neutral side-chains and thereby eliminate favorable interactions within the complex.

D38R/R39D swap (Figure 2(c))

Arg39 was identified by the FADE algorithm as being proximal to the greatest number of complementarity markers of any residue in RNase A (Table 1). With 14 atom–atom contacts to pRI, Arg39 also makes more contacts with RI than any residue in RNase A, with the exception of Glu111,

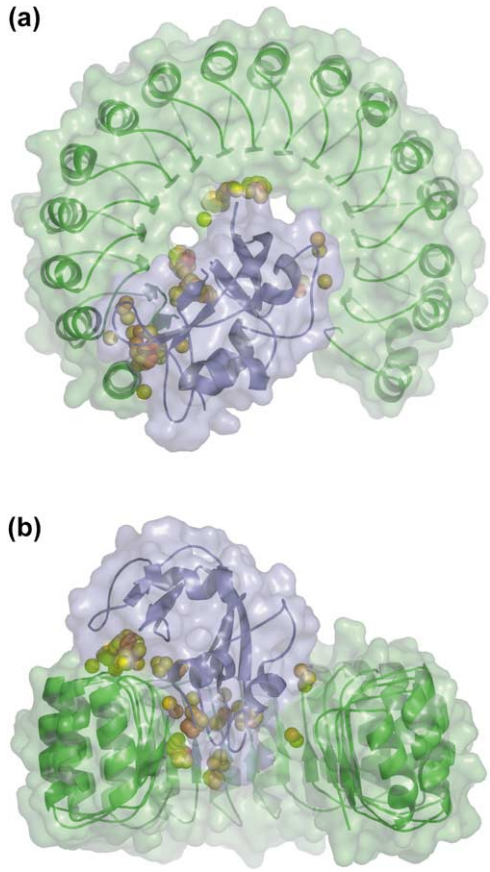

Figure 1. pRI·RNase A complex with FADE-identified shape-complementarity markers. Ribbon diagrams of pRI (green) and RNase A (blue) are shown along with their molecular surfaces. Complementarity markers identified by the FADE algorithm are represented as spheres colored on a temperature scale based on the degree of local complementarity. Red markers indicate the regions with optimal shape complementarity, and orange and yellow markers indicate regions in which the geometric match is significant, but to a lesser extent. FADE calculations and modeling were performed using the atomic coordinates from PDB entry 1DFJ.[33] The conventional view of the pRI·RNase A complex is shown in (a), and is rotated 90° into the plane of the page in (b). Images were created with the program PyMOL (DeLano Scientific, South San Francisco, CA).

which also makes 14 contacts.[24] Together, Asp38 and Arg39 of RNase A form three hydrogen bonds with Arg453 and Glu397 from pRI, respectively, with Arg39 interacting with Glu397 in a bidentate manner. Additionally, these two RNase A residues make van der Waals contacts with Gln426, Val428, Tyr430, and Ile455 of RI. Although Asp38 was not identified explicitly by the FADE analysis, we reasoned that by interchanging this residue with Arg39, we could disrupt three favorable interactions at the pRI·RNase A interface simultaneously. Moreover, the D38R/R39D swap was conservative, in that it preserved the local amino acid content.

β4–β5 loop (Figure 2(d))

Four surface loops of RNase A contribute 16 of the 24 residues that contact RI.[24] The β4–β5 loop of RNase A, containing residues 87–96, packs against an especially hydrophobic region of pRI defined by three tryptophan residues: Trp257, Trp259, and Trp314. Three RNase A residues within this loop, Gly88, Ser89, and Lys91, were identified by FADE as being important for mediating shape complementarity with RI. Earlier attempts to create an RI-evasive RNase A showed the replacement of Gly88 (FADE cluster size 5) with an arginine residue to be extremely effective at introducing steric and electrostatic strain, increasing the K_d value of the pRI·RNase A complex by nearly four orders of magnitude.[28] Therefore, although residues Ser89 and Lys91 were identified by the FADE algorithm as being near large complementarity clusters, we assumed this region of the complex to be disrupted maximally by the G88R substitution and hence did not pursue further alteration of this loop.

N67R substitution (Figure 2(a))

Asn67 was proximal to the third largest cluster of complementarity markers, following Arg39 and residues of the β4–β5 loop of RNase A. Asn67 makes six contacts with pRI residues Cys404, Val405, Gly406, and Tyr433, including a hydrogen bond with the main-chain oxygen atom of Val405. It is noteworthy that Tyr433 of pRI, which makes contacts with Asn67 of RNase A, was identified as being proximal to the largest number of complementarity markers of any residue in either protein. In accordance, Camacho and co-workers identified Tyr433 of RI and Asn67 of RNase A as the "anchor residues" in the pRI·RNase A complex.[37]

Other FADE-identified residues

Lys7 (Figure 2(b)) was the lowest scoring of the RNase A residues with a complementarity cluster size of 2. Nonetheless, Lys7 makes seven atom–atom contacts with Ser456 of pRI, including one hydrogen bond. Previous studies had shown this residue to contribute significantly to complex stability.[29,38] We also examined Asn24 and Lys31, which make seven and four atom–atom contacts and are located near cluster sizes of 5 and 2, respectively. Asn24 makes seven van der Waals contacts and two hydrogen bonds with Asp89 and Asp117 of RI; Lys31 makes three atom–atom contacts with His6 of pRI and one contact with Asp31.

Catalytic activity

A ribonuclease must retain its catalytic activity to be cytotoxic.[39] Accordingly, the catalytic activity of each ribonuclease was assayed to determine if any of the amino acid substitutions compromised cytotoxicity by reducing the ability of the enzyme

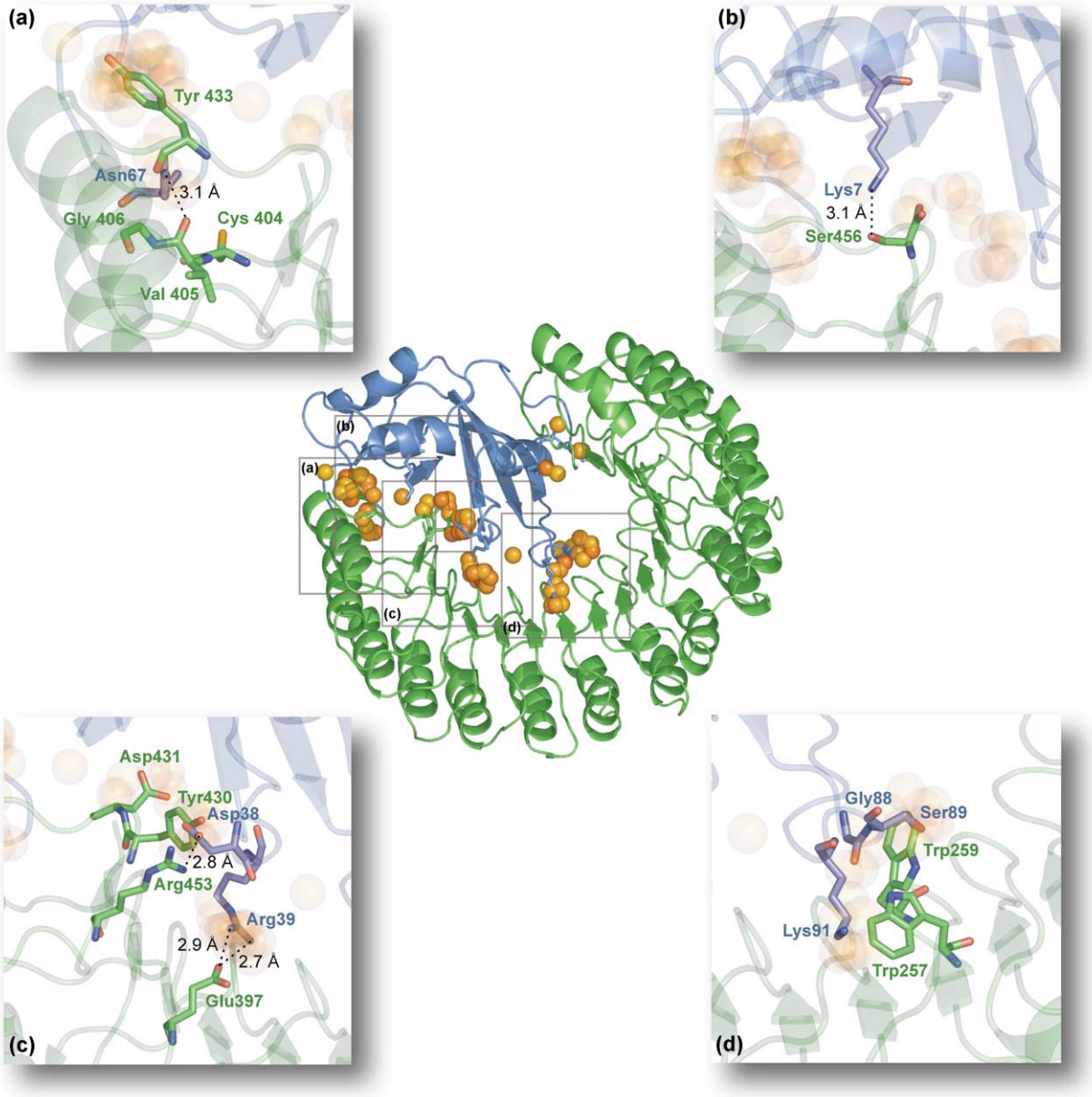

Figure 2. Regions of the pRI·RNase A interface targeted for disruption. Depictions were created as in Figure 1. The side-chains of residues proximal to shape-complementarity clusters (Table 1) are shown as sticks in the color of their protein. Interface regions of interest are shown in greater detail in (a)–(d), along with relevant interprotein hydrogen bonds.

to degrade RNA. Values of k_{cat}/K_M for wild-type RNase A, its variants, and ONC are given in Table 2. The k_{cat}/K_M values of wild-type RNase A, G88R RNase A, K7A/G88R RNase A, and ONC were $5.2\times10^7\ M^{-1}\ s^{-1}$, $7.4\times10^7\ M^{-1}\ s^{-1}$, $5.3\times10^6\ M^{-1}\ s^{-1}$, and $2.2\times10^5\ M^{-1}\ s^{-1}$, respectively, which are in good agreement with values reported previously.[29,40] Swapping residues 38 and 39 of RNase A had a minor effect on catalysis by the enzyme. The value of k_{cat}/K_M for D38R/R39D RNase A was $1.8\times10^7\ M^{-1}\ s^{-1}$, which represents only a threefold loss in ribonucleolytic activity. A similarly small effect was seen in the D38R/R39D/G88R variant; its k_{cat}/K_M value of $3.1\times10^7\ M^{-1}\ s^{-1}$ was 2.5-fold less than that of G88R RNase A. Interestingly, when the single R39D substitution was made in the context of the G88R substitution, the effect on ribonucleolytic activity was more pronounced, reducing the k_{cat}/K_M value of G88R RNase A by 17-fold to $4.3\times10^6\ M^{-1}\ s^{-1}$. This decrease could result from enhanced negative charge in this region, possibly reducing the number of productive collisions between the enzyme and its anionic substrate.

The P2 substrate binding site of RNase A, which contains Lys7, plays an important role in catalysis by RNase A.[41–43] Consistent with previous results,[29] K7A/G88R RNase A displayed an almost tenfold

Table 1. Residues of highest shape complementarity in the pRI·RNase A complex as identified with the FADE algorithm

Chain	Residue	Cluster size[a]
RNase A	Lys7	2
	Asn24	5
	Gln28	3
	Lys31	2
	Arg39	31
	Asn67	6
	Gly88	5
	Ser89	14
	Lys91	9
RI	Tyr430	22
	Asp431	10
	Tyr433	38

[a] Number of FADE complementarity markers within 2 Å of an atom in the indicated residue.

decrease in ribonucleolytic activity, having a k_{cat}/K_M value of $5.3\times10^6\ M^{-1}\ s^{-1}$. This deleterious contribution to catalysis was additive when combined with other amino acid substitutions that diminished activity; the D38R/R39D swap (three-fold decrease in k_{cat}/K_M) when combined with the K7A substitution (tenfold decrease in k_{cat}/K_M) resulted in a K7A/D38R/R39D variant with an activity of $1.6\times10^6\ M^{-1}\ s^{-1}$, which is 30-fold less than that of wild-type RNase A. Additionally, the K7A substitution was responsible for a 15-fold reduction in the activity of D38R/R39D/G88R RNase A, reducing the activity of the quadruple variant K7A/D38R/R39D/G88R RNase A to $1.6\times10^6\ M^{-1}s^{-1}$.

The majority of the FADE-inspired substitutions had no significant effect on ribonucleolytic activity. The N67R, K31A, and N24R substitutions, when combined individually with the G88R substitution, produced enzymes with catalytic activity roughly comparable to that of G88R RNase A itself. Values of k_{cat}/K_M for these three variants were $9.2\times10^7\ M^{-1}\ s^{-1}$, $5.2\times10^7\ M^{-1}\ s^{-1}$, and $7.8\times10^7\ M^{-1}\ s^{-1}$, respectively. Therefore, RNase A variants combining many of these substitutions (such as K31A/D38R/R39D/N67R/G88R RNase A and D38R/R39D/N67R/G88R RNase A) possessed nearly the k_{cat}/K_M value of the wild-type enzyme ($4.8\times10^7\ M^{-1}\ s^{-1}$and $3.8\times10^7\ M^{-1}\ s^{-1}$, respectively).

Table 2. Biochemical parameters and cytotoxic activities of RNase A, its variants, and ONC

Ribonuclease	T_m[a] (°C)	k_{cat}/K_M[b] ($10^6\ M^{-1}\ s^{-1}$)	K_d (pRI) (nM)[c]	$\Delta\Delta G$[d] (pRI) (kcal/mol)	K_d[e] (hRI) (nM)	$(k_{cat}/K_M)_{cyto}$ ($10^6\ M^{-1}\ s^{-1}$)[f]	IC_{50} (μM)[g]
Wild-type RNase A	64	52±4	67×10^{-6}[h]	–	44×10^{-6}[i]	57×10^{-6}	>25
D38R/R39D RNase A	60	18±3	0.30±0.01	5.0	0.50±0.09	0.0022	>25
N67R RNase A	57	73±19	0.36±0.01	5.1	ND	–	>25
K7A/D38R/R39D RNase A	62	1.6±0.1	3.5	6.4	ND	–	17±5
N24R/G88R RNase A	60	78±5	0.27	4.9	ND	–	8.4±0.7
G88R RNase A	60[j]	74±4	0.57±0.05[k]	5.3	1.2±0.2	0.022	4.6±0.4
K31A/G88R RNase A	ND	52±2	ND	ND	57±3	0.74	1.5±0.2
K7A/G88R RNase A	62[l]	5.3±0.4	17±1	7.4	62±6	0.080	1.1±0.1
R39D/G88R RNase A	61	4.3±1	ND	ND	870±40	0.77	0.69±0.07
N67R/G88R RNase A	58	92±4	45±2	8.0	3.8±0.2	0.090	0.51±0.05
K7A/D38R/R39D/G88R RNase A	60	1.6±0.2	120±10	8.5	$(2.9\pm0.2)\times10^3$	0.67	0.41±0.05
ONC	90[m]	0.22±0.01	$\geqq10^3$	–	$\geqq10^3$	–	0.27±0.02
D38R/R39D/G88R RNase A	60	31±3	8.0±0.4	6.9	90±3	0.69	0.22±0.04
K31A/D38R/R39D/N67R/G88R RNase A	54	48±7	ND	–	$(2.5\pm0.3)\times10^3$	18	0.21±0.06
D38R/R39D/N67R/G88R RNase A	56	38±6	$(1.4\pm0.1)\times10^3$	10.0	510±30	4.3	0.19±0.02

ND, not determined.

[a] Values of T_m (±2 deg. C) for RNase A and its variants were determined in PBS by UV spectroscopy.

[b] Values of k_{cat}/K_M (±SE) for RNase A and its variants are for catalysis of 6-FAM-dArU(dA)$_2$-6-TAMRA cleavage at 23(±2) °C in 0.10 M Mes–NaOH buffer (OVS-free) at pH 6.0, containing 0.10 M NaCl. The value of k_{cat}/K_M (±SE) for ONC is for catalysis of 6-FAM-dArUdGdA-6-TAMRA cleavage at 23(±2) °C in 0.020 M Mes–NaOH buffer (OVS-free) at pH 6.0, containing 0.010 M NaCl.

[c] Values of K_d (±SE) are for the complex with pRI at 23(±2) °C. The K_d value for ONC is an estimate.[9]

[d] Values of $\Delta\Delta G$ were calculated with the equation: $\Delta\Delta G = -RT\ \ln(K_d^{wild-type}/K_d^{variant})$.

[e] Values of K_d (±SE) are for the complex with hRI at 23(±2) °C.

[f] Values of $(k_{cat}/K_M)_{cyto}$ were calculated with equation (1) and values of K_d for the complex with hRI.

[g] Values of IC_{50} (±SE) are for incorporation of [*methyl*-^{3}H]thymidine into the DNA of K-562 cells exposed to a ribonuclease, and were calculated with equation (3).

[h] From Vicentini *et al.*[25]

[i] From Lee *et al.*[57]

[j] From Leland *et al.*[28]

[k] From Abel *et al.*[65]

[l] From Haigis *et al.*[29]

[m] From Leland *et al.*[28] and determined by circular dichroism spectroscopy.

Affinity for ribonuclease inhibitor

The amino acid sequences of pRI and hRI are quite similar (77% identity). Moreover, of the 28 residues in pRI that contact RNase A,[44] only two are replaced by dissimilar residues in hRI. Despite the assumption that the two inhibitor proteins would possess similar affinities for the RNase A variants, we determined the K_d values of complexes with both pRI and hRI. These K_d values are given in Table 2.

As a rigorous test of the utility of the FADE algorithm for identifying residues important for protein–protein interactions, we determined the K_d values of the FADE-inspired variants in complexes with pRI. The K_d values of 0.57 nM and 17 nM obtained for G88R RNase A and K7A/G88R RNase A in complexes with pRI, were in good agreement with those determined previously.[29] The N24R substitution was the only change that did not diminish the affinity of pRI for RNase A. Indeed, with a K_d value of 0.27 nM, N24R/G88R RNase A actually appeared to form a slightly tighter complex with pRI than did G88R RNase A. The most significant increases in values of K_d were observed for the D38R/R39D swap and the N67R substitution, whose complexes exhibited K_d values of 0.30 nM and 0.36 nM, respectively. These amino acid changes were responsible for 4500-fold and 5400-fold increases in K_d value, respectively. The K7A/D38R/R39D, N67R/G88R, and D38R/R39D/G88R variants formed complexes with pRI that have K_d values of 3.5 nM, 45 nM, and 8.0 nM, respectively.

The combination of multiple substitutions produced the most RI-evasive variants of RNase A. Of note are the K7A/D38R/R39D/G88R and D38R/R39D/N67R/G88R variants, which formed complexes with pRI having K_d values of 0.12 μM and 1.4 μM, respectively. Notably, D38R/R39D/N67R/G88R RNase A is the first RNase A variant observed to form a complex with pRI that has a micromolar K_d value. By changing only four out of 124 residues in RNase A, the K_d value of the pRI·RNase A complex was increased by 20×10^6-fold with the D38R/R39D/N67R/G88R variant.

Values of K_d for the complexes of pRI with RNase A variants are ideal for assessing the ability of the FADE algorithm to identify shape-complementarity markers. As a chemotherapeutic agent, however, cytotoxic ribonucleases must be capable of eluding human RI. For this reason, values of K_d were also determined for the hRI complexes with RNase A variants. With the exception of two variant RNase A variants, K_d values for the hRI complexes were greater than those obtained for pRI, with the magnitude of the differences ranging from twofold to 24-fold. The highest K_d value observed for a complex with hRI was that of K7A/D38R/R39D/G88R RNase A at 2.9 μM, which represents a 60×10^6-fold decrease in affinity for hRI.

Importantly, the destabilizing effects of these substitutions on the complex were not entirely additive, indicating that the pRI·RNase A interface is plastic. The accommodating nature of the binding interface can be seen upon comparison of $\Delta\Delta G$ values (Table 2). For example, the G88R and N67R substitutions destabilize the complex by approximately 5 kcal/mol each. Yet, the N67R/G88R double variant exhibits an 8 kcal/mol loss in binding free energy, despite the spatial separation of these two substitutions. Chen and Shapiro had previously described multiple changes made in hRI as having sub-additive effects on complex destabilization.[45] They explained this negative cooperativity as a result of a broad distribution of binding energy over a large interface.[45] Our results support this observation.

Conformational stability

The conformational stability of a ribonuclease is necessary for biological function, including cytotoxicity.[46] Hence, the T_m value of each RNase A variant was determined and is given in Table 2. The N67R substitution was the most destabilizing, decreasing the T_m value of wild-type RNase A by 7 deg. C to a value of 57 °C. This loss in conformational stability was not recovered by additional substitutions, being observed in all variants containing the N67R substitution. The N67R/G88R and D38R/R39D/N67R/G88R variants had T_m values of 58 °C and 56 °C, respectively. K31A/D38R/R39D/N67R/G88R RNase A had the lowest T_m value of 54 °C, which is nearly 10 deg. C lower than that of the wild-type enzyme. Still, this T_m value is significantly greater than physiological temperature. None of the other amino acid substitutions reduced the T_m value by more than a few deg. C.

Cytotoxicity

The toxicity of each ribonuclease was measured with the K-562 human leukemia cell line. Ribonucleases are given in order of increasing cytotoxicity in Table 2, using IC_{50} values derived by applying equation (3) to the data in Figure 3 ($h=1.43\pm0.02$ for the 12 cytotoxic ribonucleases). ONC, G88R RNase A, and K7A/G88R RNase A displayed IC_{50} values similar to those reported previously.[28,29,47] D38R/R39D RNase A (Figure 3(a)) and N67R RNase A (Figure 3(c)) exhibited no cytotoxic activity, even at concentrations of 25 μM. The lack of cytotoxicity for the latter two variants is interesting, considering the large increase in cytotoxicity they exhibited in the context of the G88R substitution.

Upon incorporation of the K7A substitution into the D38R/R39D/G88R variant, its affinity for hRI decreased 32-fold, consistent with the loss of favorable interactions between the lysine side-chain and C-terminal serine residue of hRI. This larger K_d value was accompanied by a loss in catalytic activity, leading to an IC_{50} value nearly twice that of D38R/R39D/G88R RNase A. Although Asp38 was not identified explicitly by

the FADE analysis, its importance in the conservative D38R/R39D swap is apparent when the IC_{50} value of R39D/G88R RNase A ($IC_{50}=0.69$ μM) is compared with that of D38R/R39D/G88R RNase A ($IC_{50}=0.22$ μM).

Two of the most cytotoxic variants of RNase A discovered in this work, D38R/R39D/G88R and D38R/R39D/N67R/G88R, as well as ONC, wild-type RNase A, and G88R RNase A, were screened for cytotoxic activity against ten different cell lines. The resulting IC_{50} values of these ribonucleases are listed in Table 3. All of the cell lines are of human origin, except for NmuMG, which is a mouse mammary normal epithelial cell line. With the exception of the Hep3B cell line, all of the human cancer cell lines, like the human leukemia K-562 line, are among the 60 cell lines screened by the National Cancer Institute in search of novel cancer chemotherapeutic agents.

The cell lines are given in Table 3 according to increasing doubling times. There did not appear to be any direct correlation between doubling time and sensitivity to the ribonucleases as had been reported previously.[22] In general, the trend of cytotoxicity among the RNase A variants reflected that seen in the K-562 cell line, namely D38R/R39D/N67R/G88R > D38R/R39D/G88R > G88R > wild-type RNase A, with the D38R/R39D/N67R/G88R variant consistently having the lowest IC_{50} value. The HCT-116, A549, and SF268 cell lines were exceptions to this general trend, as all were more sensitive to wild-type RNase A than was G88R RNase A. Batra and co-workers have reported that wild-type human pancreatic ribonuclease (RNase 1) is toxic to some cell lines,[48] just as we found several cell lines susceptible to wild-type RNase A. These three cell lines derive from three different tissue types: colon, lung, and central nervous system, respectively.

A goal of this research was to develop RNase A variants possessing cytotoxicity equal to or greater than that of ONC. This goal was achieved with the D38R/R39D/N67R/G88R variant in the K-562, Du145, Hep-3B, and SF268 cell lines. In the remaining six cell lines, ONC exhibited threefold to 30-fold greater cytotoxicity than did the RNase A

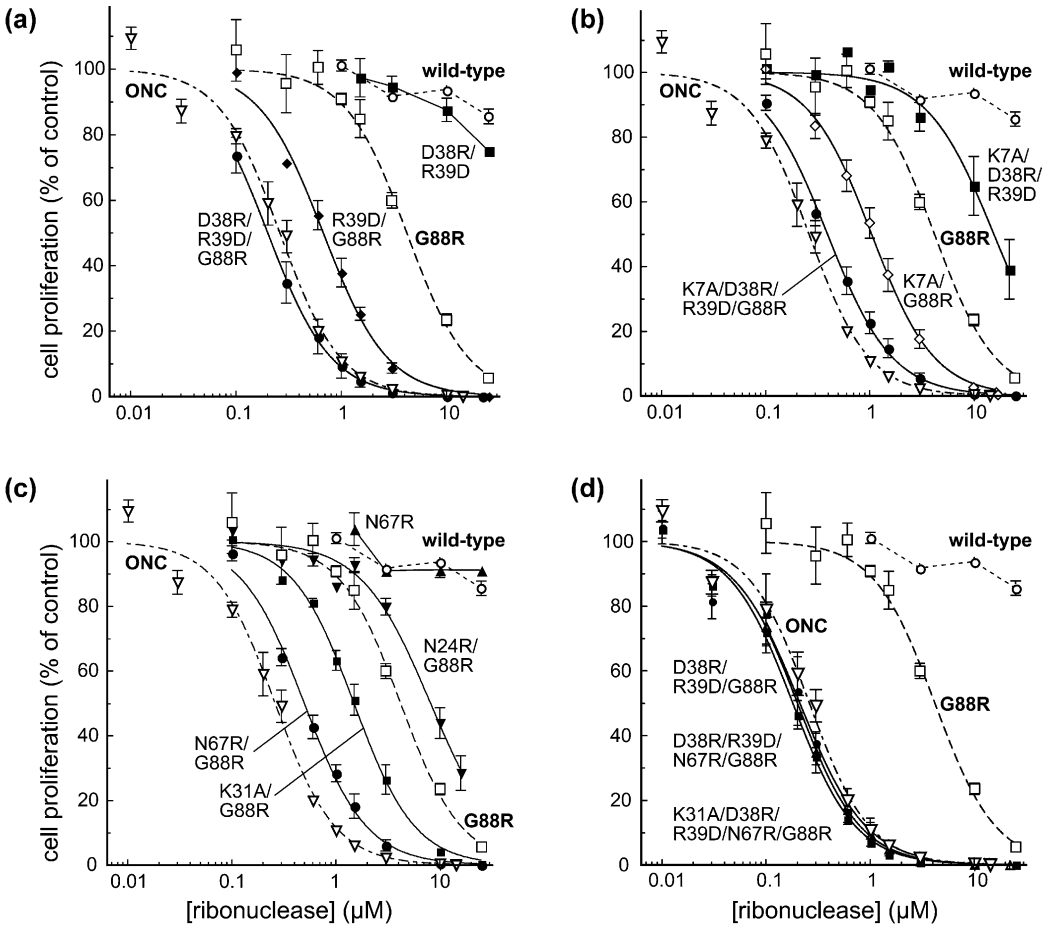

Figure 3. Effect of ribonucleases on the proliferation of K-562 cells. The incorporation of [*methyl*-^{3}H]thymidine into cellular DNA was used to monitor the proliferation of K-562 cells in the presence of ribonucleases. Data points indicate the mean (±SE) of at least three separate experiments carried out in triplicate. In each panel, data for wild-type RNase A, G88R RNase A, and ONC, are shown as open symbols with curves fitted as broken lines. (a) Effect of the D38R/R39D swap. (b) Effect of the K7A substitution. (c) Effect of additional FADE-inspired substitutions in the context of G88R, including N24R, K31A, and N67R. (d) Compilation of data for variants with cytotoxicity greater than that of ONC.

Table 3. IC_{50} values of RNase A, its variants, and ONC for ten cell lines

Cell line	Description	Doubling time (h)	IC_{50}[a] (μM)				
			Wild-type	DRNG[b]	DRG[b]	G88R	ONC
HCT-116	Colon carcinoma	17.4	4.7	0.49	1.4	10.4	0.14
NCI-H460	Lung carcinoma	17.8	39	0.71	0.60	11.0	0.13
A549	Lung adenocarcinoma	22.9	15.5	4.8	13.7	27.0	0.15
MCF-7	Breast adenocarcinoma	25.4	21.7	0.27	0.42	4.4	0.086
Du145	Prostate carcinoma	32.3	5.5	0.085	0.45	2.0	0.11
SF-268	CNS glioblastoma	33.1	3.8	0.18	0.64	4.6	0.088
NCI/ADR-RES	Breast adenocarcinoma	34.0	19	1.00	2.3	5.8	0.06
SK-OV-3	Ovary adenocarcinoma	48.7	3.2	0.76	1.5	2.8	0.13
Hep-3B	Liver carcinoma	ND	2.8	0.031	0.040	0.34	0.051
NmuMG	Mammary normal epithelial (mouse)	ND	>40	>10	>20	>40	1.6

[a] Values of IC_{50} are for the conversion of calcein AM to calcein in cells exposed to a ribonuclease, and were calculated with equation (4).
[b] DRNG and DRG refer to the D38R/R39D/N67R/G88R and D38R/R39D/G88R variants of RNase A, respectively.

variants. Interestingly, none of the RNase A-derived variants tested in this screen was toxic to the normal cell line NmuMG at the maximum concentrations tested. This discrimination was not observed with ONC, which had an IC_{50} of 1.62 μM for the normal mouse cell line.

Discussion

ONC and BS-RNase exhibit natural cytotoxic activity, an attribute due, in part, to their ability to evade RI.[3–5,49] RNase A is bound tightly by RI and lacks cytotoxicity. We showed previously that diminishing the affinity of RNase A for RI enables the enzyme to degrade cellular RNA and elicit cell death.[28,29,50] Encouraged by these results, we set out to unleash the full cytotoxic potential of RNase A by more thoroughly disrupting its interaction with RI.

An atypical interface

Proper biological function requires macromolecules to interact with specific recognition and appropriate affinity. There are many properties of a protein–protein interface that can endow the complex with stability, including total surface area, non-polar surface area, packing density, and polar interactions.[51] The 2550 $Å^2$ of solvent-accessible surface area buried upon formation of the pRI·RNase A complex is relatively large for an enzyme·inhibitor complex, and is considerably larger than the 1600 $Å^2$ that is typical for protease·inhibitor complexes.[52] In general, protein interfaces resemble the chemical character of solvent-exposed protein surfaces, which are comprised of approximately 57% non-polar, 24% neutral polar, and 19% charged amino acid residues.[53] Typical protein–protein interfaces do, however, contain fewer charged residues and more neutral polar residues than do solvent-exposed protein surfaces. Deviating from this trend, the pRI–RNase A interface is significantly more charged, with 49% non-polar, 27% neutral polar, and 24% charged residues.[24] Indeed, electrostatics seem to play an important role in the complex formed between the basic RNase A (pI 9.3)[54] and the acidic RI protein (pI 4.7)[24] at cytosolic pH.

In contrast to the larger role of charge–charge interactions within the pRI·RNase A complex, the degree of shape complementarity between the two surfaces is lower than average. The shape correlation statistic, S_c, describes how well two surfaces mesh, with a value of 1.0 describing a perfect match and 0.0 describing two unrelated surfaces.[55] The pRI·RNase A interface has a relatively low S_c value of 0.58,[33] as compared to values of 0.70–0.76 for typical protease·inhibitor complexes and 0.64–0.68 for typical antibody·antigen complexes.[55] The packing of atoms at the pRI–RNase A interface is also less dense than a typical protein interior or protein–protein interface.[51] The large amount of buried surface area could compensate for the relatively low degree of shape complementarity, to yield the highly stable interaction between RI and RNase A.

Disrupting the RI·RNase A complex

Prior to this work, K7A/K41R/G88R RNase A was the most RI-evasive of known variants.[29] This variant formed a complex with pRI that had a K_d value of 47 nM, nearly 10^2-fold greater than that of G88R RNase A. Still, K7A/K41R/G88R RNase A is not a potent cytotoxin, owing largely to the 10^2-fold decrease in ribonucleolytic activity caused by the replacement of its active-site lysine residue with arginine.[47,50,56]

The FADE algorithm revealed new "knobs" and "holes" in the pRI·RNase A complex for disruption by site-directed mutagenesis (Figures 1 and 2; Table 1). In the RNase A variants created in this work, the D38R/R39D swap and N67R substitution produced the largest decrease in affinity for RI. Alone, each of these substitutions effected a destabilization of the pRI·RNase A complex nearly equal to that of the G88R substitution.[28] Combining the most disruptive FADE-inspired substitutions resulted in ribonucleases that were 30-fold more RI-evasive than K7A/K41R/G88R RNase A, and

retained nearly wild-type catalytic activity (Table 2). Moreover, the D38R/R39D/G88R, D38R/R39D/N67R/G88R, and K31A/D38R/R39D/N67R/G88R variants were all more cytotoxic to K-562 cells than was ONC (Figure 3).

One interesting finding is the difference in affinity of the porcine and human homologs of RI observed for some of the RNase A variants. In general, RNase A variants were bound more tightly by pRI than hRI (Table 2). This higher affinity of pRI for RNase A was not observed when the equilibrium dissociation constants were measured originally for complexes of wild-type RNase A with pRI ($K_d = 6.7\times10^{-14}$ M)[25] and hRI ($K_d = 4.4\times10^{-14}$ M).[57] Of the 28 pRI residues that contact RNase A, 25 are identical in hRI. The three differences among the RNase A binding residues are the replacements of His6 in pRI with a glutamine residue in pRI, Asp228 with alanine, and Val405 with leucine.[58] All three of these pRI residues make atom–atom contacts exclusively with FADE-identified RNase A residues. His6 makes three contacts with Lys31 of RNase A, Asp228 makes two contacts with Ser89, and Val405 makes three contacts with Asn67. These three changes are likely to contribute to the differential affinity of pRI and hRI for the RNase A variants.

RI evasion as a molecular determinant of cytotoxicity

Several factors have been shown to be important molecular determinants for ribonuclease cytotoxicity, including catalytic activity[39] and evasion of RI.[22] We unified the impact of these two parameters with the equation:

$$(k_{cat}/K_M)_{cyto} = \frac{k_{cat}/K_M}{1 + [RI]/K_d} \quad (1)$$

In equation (1), the parameter $(k_{cat}/K_M)_{cyto}$ reports on the activity of a ribonuclease in the cytosol, which contains RI at an invariant concentration of ~4 μM.[21,22,59] Although equation (1) does not take into account important properties such as cationic charge and conformational stability, we and others have found that equation (1) is a useful forecaster of ribonuclease cytotoxicity.[29,47,50,60,61]

In general, the cytotoxic activities of the RNase A variants in Table 2 correlate well with their $(k_{cat}/K_M)_{cyto}$ values. One exception to the predictive ability of equation (1) is R39D/G88R RNase A. With a $(k_{cat}/K_M)_{cyto}$ value of 2.6×10^6, we expected this variant to be more toxic to K-562 cells than was observed herein. Molecular charge is likely responsible for the anomaly. Replacing Arg39 with an aspartate residue decreases catalytic activity by tenfold, and reduces the net charge by 2. The lower charge could diminish endocytosis of the protein and thus account for its lowered cytotoxicity, as has been observed for other ribonuclease variants.[5,61–63]

The relationship between IC_{50} and $(k_{cat}/K_M)_{cyto}$ is depicted in Figure 4. The value of $(k_{cat}/K_M)_{cyto}$ is

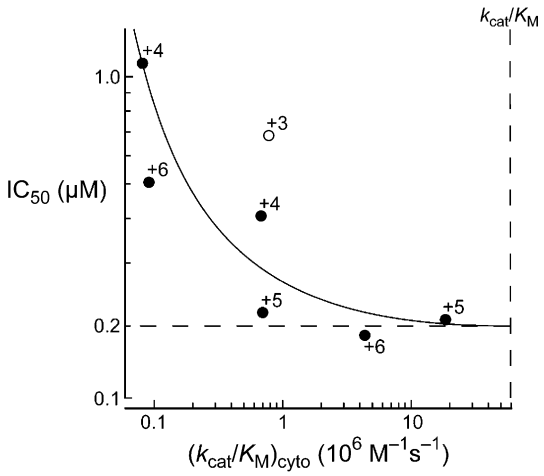

Figure 4. Relationship of $(k_{cat}/K_M)_{cyto}$ and cytotoxicity. IC_{50} values of RNase A variants for K-562 cells are plotted against their $(k_{cat}/K_M)_{cyto}$ values (Table 2). Each point represents an individual RNase A variant with $IC_{50} <$ 1.1 μM. Both axes have a log scale. The broken line at 0.2 μM indicates the apparent upper limit of the cytotoxicity attainable against this cell line by enhancing RI evasion.

constrained by equation (1) to be less than $k_{cat}/K_M = 5\times10^7$ M^{-1} s^{-1}, which refers to the ribonucleolytic activity of wild-type RNase A. The vertical broken line in Figure 4 depicts this uppermost value. The horizontal dotted line reflects what appears to be the lowest IC_{50} value that could be achieved by improving RI evasion alone. The variants in the upper left quadrant of the plot show a distinct decrease in IC_{50} value with increasing $(k_{cat}/K_M)_{cyto}$ value. The only outlier to this trend is R39D/G88R, which has a lower molecular charge (*vide supra*). As the $(k_{cat}/K_M)_{cyto}$ value reaches ~5×10^6 M^{-1} s^{-1}, the trend levels off, with little further increases in cytotoxicity. Thus, we believe we have exhausted the improvements in cytotoxicity that can be achieved *via* RI evasion alone. A further reduction in IC_{50} value is likely to be achievable, but only by altering other features of the pathway leading to cell death.

Utility of the FADE algorithm

We used the FADE algorithm to identify quickly and objectively RNase A residues within the pRI·RNase A complex that exhibit a high degree of shape complementarity. Several of the residues identified by the FADE algorithm were previously shown experimentally to contribute a significant amount of binding energy to the pRI·RNase A complex,[38,58] or to be excellent targets for disruption by mutagenesis.[28,29] The success of the FADE algorithm in predicting the importance of these regions gave credence to its utility and justified our subsequent analysis of additional RNase A residues identified by FADE. Although a similar list of

residues could have been identified by careful examination of the three-dimensional structure, the evident advantage of FADE is the extreme speed at which it identifies regions of high complementarity. Additionally, the computational algorithm is objective, eliminating possible human error or bias.

Therapeutic index

An important characteristic of any drug is its therapeutic index (TI), which is the ratio of its toxic dose to its effective dose. In humans, ONC exhibits a highly favorable TI as a cancer chemotherapeutic agent, enabling its progress to phase III clinical trials.[10] Mammalian ribonucleases could exhibit an even greater TI than does ONC. For example, the Hep-3B liver carcinoma cell line is the most vulnerable to all of the ribonucleases tested herein (Table 3). ONC has a TI, defined here as $IC_{50}^{NmuMG}/IC_{50}^{Hep-3B}$, of 31. In contrast, the D38R/R39D/N67R/G88R, D38R/R39D/G88R, and G88R variants of RNase A have TI values of >323, >500, and >118, respectively. A biochemical explanation for the TI of ribonucleases (amphibian or mammalian) awaits further experimentation.

Conclusions

On the basis of the results presented here, we conclude that the FADE algorithm is an effective tool for identifying residues at the interface of a protein–protein complex that can be altered to disrupt the complex. Such alterations to RNase A reduce its affinity for RI, and thus increase its cytotoxicity. Some of these variants of RNase A are more toxic to cancer cells than is its amphibian homolog ONC, and thus represent a landmark on the path to the development of chemotherapeutic agents based on mammalian ribonucleases.

Materials and Methods

Materials

Escherichia coli BL21(DE3) cells and pET22b(+) and pET27b(+) plasmids were from Novagen (Madison, WI). K-562 cells were derived from a continuous human chronic myelogenous leukemia line obtained from the American Type Culture Collection (Manassas, VA). Cell culture medium and supplements were from Invitrogen (Carlsbad, CA). [*methyl*-^{3}H]Thymidine (6.7 Ci/mmol) was from Perkin–Elmer (Boston, MA). Enzymes were obtained from Promega (Madison, WI) or New England Biolabs (Beverly, MA). Ribonuclease substrates 6-FAM-dArUdAdA-6-TAMRA and 6-FAM-dArUdGdA-6-TAMRA were from Integrated DNA Technologies (Coralville, IA). All other chemicals used were of commercial reagent grade or better, and were used without further purification.

Terrific Broth (TB) contained (in 1.00 l) 12 g of Tryptone, 24 g of yeast extract, 4 ml of glycerol, 2.31 g of KH_2PO_4, and 12.54 g of K_2HPO_4. Phosphate-buffered saline (PBS) contained (in 1.00 l) 8.0 g of NaCl, 2.0 g of KCl, 1.15 g of $Na_2HPO_4{\cdot}7H_2O$, 2.0 g of KH_2PO_4, and 0.10 g of NaN_3, and had pH 7.4.

Analytical instruments

[*methyl*-^{3}H]Thymidine incorporation into K-562 genomic DNA was quantified by scintillation counting using a Microbeta TriLux liquid scintillation and luminescence counter (Perkin–Elmer, Wellesley, MA). The mass of each protein variant was confirmed by matrix-assisted laser desorption/ionization time-of-flight (MALDI-TOF) mass spectrometry using a Voyager-DE-PRO Biospectrometry Workstation (Applied Biosystems, Foster City, CA). Fluorescence measurements were made with a QuantaMaster1 photon-counting fluorimeter equipped with sample stirring (Photon Technology International, South Brunswick, NJ). Thermal denaturation data were acquired using a Cary 3 double-beam spectrophotometer equipped with a Cary temperature-controller (Varian, Palo Alto, CA).

Design of ribonuclease A variants

The FADE program calculates shape-complementarity markers of proteins at complex interfaces. Atomic density[64] is measured using fast Fourier transform algorithms based on methods described previously.[30] Using the structure of the crystalline pRI·RNase A complex (PDB entry 1DFJ),[33] critical RNase A residues in close proximity to large clusters of shape-complementarity markers were identified and are given in Table 1. Amino acid substitutions were chosen to create maximal electrostatic or steric conflict as well as eliminate any favorable Coulombic or short-range interactions.

At the onset of this research, the most cytotoxic variant of RNase A known was K7A/G88R RNase A.[29] Subsequent amino acid substitutions inspired by FADE analysis were made initially in the background of these established changes, with the expectation that any additional contributions to evasivity would be additive. As discussed here, we found that the loss of enzymatic activity accompanying the K7A substitution compromised cytotoxicity, and hence, later substitutions were made in the background of the G88R substitution alone. The G88R background provided a well-characterized benchmark of cytotoxicity and RI-evasion from which we could identify improvements using our established assays.[28,65] Substitutions that were successful in the G88R background were also made alone to assess their individual contribution to evasion of RI and cytotoxicity.

Production of ribonucleases

cDNA encoding RNase A variants was created by oligonucleotide-mediated site-directed mutagenesis[66] using a pET22b(+) or pET27b(+) plasmid that contained cDNA encoding wild-type RNase A or its G88R variant, respectively.[28] ONC, wild-type RNase A, and RNase A variants were produced as described,[28,67] with the following exceptions. Inclusion bodies from *E. coli* were stirred in 20 mM Tris–HCl (pH 8.0), 7 M guanidine–HCl, 0.1 M DTT, and 10 mM EDTA until dissolved thoroughly. Ribonucleases were refolded overnight at room temperature following slow dilution into 0.10 M Tris–HCl (pH 8.0), 0.1 M NaCl, 1.0 mM reduced glutathione, and 0.2 mM oxidized glutathione. Following purification,

proteins were dialyzed against PBS and filtered (0.2 μm pore size) prior to use in biochemical assays. Protein concentration was determined by UV spectroscopy using an extinction coefficient of $\epsilon_{278} = 0.72$ mg ml^{-1} cm^{-1} for RNase A and its variants,[68] and $\epsilon_{280} = 0.87$ mg ml^{-1} cm^{-1} for ONC.[28]

Production of ribonuclease inhibitors

pRI was prepared as described.[69] Freshly prepared pRI was confirmed to be 100% active by its ability to titrate the ribonucleolytic activity of wild-type RNase A.

hRI was produced in *E. coli* BL21(DE3) cells transformed with a pET22b(+) plasmid that contained cDNA encoding hRI between its NdeI and SalI sites. Cultures (1.0 l) of TB were inoculated to an absorbance at 600 nm (A_{600}) of 0.005 from an overnight culture. The culture was grown at 37 °C to an A_{600} of 1.8–2.0. IPTG was added to a final concentration of 0.5 mM, and induction was carried out overnight at 18 °C. Subsequent purification of soluble protein and activity determination of hRI was carried out in the same manner as that used for pRI.[69]

Following purification, ribonucleases and ribonuclease inhibitor proteins migrated as single bands during SDS-PAGE, confirming their purity and apparent molecular mass. In addition, the integrity of purified ribonucleases was confirmed by MALDI-TOF mass spectrometry (Table 4).

Measurements of conformational stability

The conformational stability of the RNase A variants were assessed. Protein was dialyzed exhaustively against PBS and diluted to a concentration of ~25 μM. Assays were performed by incremental heating (0.15 deg. C/min from 25–75 °C) and measurement of the absorbance at 287 nm.[70] Data were collected and analyzed with the program THERMAL from Varian Analytical Instruments (Walnut Creek, CA).

Assays of ribonuclease inhibitor binding

The affinity of RNase A variants for both pRI and hRI was determined by using a slight modification of a competition assay reported previously.[65] Briefly, both fluorescein-labeled G88R RNase A (final concentration: 50 nM) and various concentrations of an unlabeled ribonuclease were added to 2.0 ml of PBS containing 5 mM DTT. Following incubation for 15 min at 23(±2) °C, protected from light, the initial fluorescence intensity of the unbound fluorescein-labeled G88R RNase A was monitored for 3 min (excitation at 493 nm, emission at 515 nm). pRI was then added (final concentration: 50 nM, which is sufficient to bind 90% of the fluorescein-labeled G88R RNase A in the absence of unlabeled competitor), and the final fluorescence intensity was measured. The competition assay was carried out identically for hRI. The affinity of hRI for fluorescein-labeled G88R RNase A was determined by titrating 0.8 nM fluorescein-labeled G88R RNase A with various amounts of hRI (0.026–26 nM) and recording the decrease in fluorescence upon binding. The value of K_d was found to be 1.4 nM, which is within the standard error of the value determined for unlabeled G88R RNase A (Table 2).

Table 4. Mass analysis of RNase RNase A, its variants, and ONC

Ribonuclease	Mass[a] (Da)	
	Expected	Observed
Wild-type RNase A	13,682	13,682
D38R/R39D RNase A	13,682	13,692
N67R RNase RNase A	13,724	13,711
K7A/D38R/R39D RNase A	13,625	13,630
N24R/G88R RNase A	13,824	13,833
G88R RNase A	13,781	13,785
K31A/G88R RNase A	13,724	13,723
K7A/G88R RNase A	13,724	13,726
R39D/G88R RNase A	13,740	13,741
N67R/G88R RNase A	13,824	13,829
K7A/D38R/R39D/G88R RNase A	13,724	13,735
ONC	11,820	11,825
D38R/R39D/G88R RNase A	13,781	13,793
K31A/D38R/R39D/N67R/G88R RNase A	13,766	13,765
D38R/R39D/N67R/G88R RNase A	13,824	13,825

[a] Values were determined by MALDI-TOF mass spectrometry.

Assays of catalytic activity

The ribonucleolytic activities of RNase A and its variants were determined by assaying their ability to cleave the hypersensitive fluorogenic substrate 6-FAM-dArUdAdA-6-TAMRA (20 nM), which exhibits a 180-fold increase in fluorescence (excitation at 493 nm, emission at 515 nm) upon cleavage.[71] Assays were carried out at 23(±2) °C in 2.0 ml of 0.10 M Mes–NaOH (pH 6.0), 0.10 M NaCl. The Mes used to prepare the assay buffer was purified by anion-exchange chromatography to remove trace amounts of oligomeric vinylsulfonic acid, which is a byproduct of commercial buffer synthesis and has been shown to be a potent inhibitor of RNase A.[72] Values of k_{cat}/K_M were obtained with the equation:

$$k_{cat}/K_M = \left(\frac{\Delta I/\Delta t}{I_{max} - I_0}\right)\frac{1}{[\text{ribonuclease}]} \qquad (2)$$

where $\Delta I/\Delta t$ represents the initial reaction velocity generated by cleavage of the 6-FAM-dArUdAdA-6-TAMRA substrate upon addition of ribonuclease to the cuvette. I_0 and I_{max} are, respectively, the fluorescence intensities prior to enzyme addition and following the complete cleavage of substrate by excess wild-type RNase A. Activity values for ONC were determined at 23(±2) °C in 2.0 ml of OVS-free 20 mM Mes–NaOH (pH 6.0), 0.010 M NaCl using 20 nM 6-FAM-dArUdGdA-6-TAMRA.[40]

Assays of cytotoxicity

IC_{50} values for RNase A, its variants, and ONC were determined by measuring the incorporation of [*methyl*-^{3}H]thymidine into the cellular DNA of K-562 cells in the presence of ribonucleases as described.[28] All cytotoxicity assays were repeated at least three times in triplicate. Each data point represents the mean of three or more experimental values (±SE). IC_{50} values were calculated by fitting the curves using non-linear regression to a sigmoidal dose–response curve with the equation:

$$y = \frac{100\%}{1 + 10^{(\log(IC_{50}) - \log[\text{ribonuclease}])h}} \qquad (3)$$

In equation (3), y is the total DNA synthesis following a 4 h [*methyl*-^{3}H]thymidine pulse, and h is the slope of the curve.

Cytotoxicity assays other than those carried out using K-562 cells were performed at the Keck–UWCCC Small Molecule Screening Facility. These assays used ten cell lines from a broad spectrum of tissues. Following incubation with ribonucleases for 72 h, IC_{50} values were determined by measuring the enzymatic conversion of the profluorophore calcein AM (Molecular Probes, Eugene, OR) to calcein in live cells. Coefficient of variation and *Z*-scores[73] were determined for each cell line using doxorubicin as an internal control. All cytotoxicity assays were performed in triplicate three times. IC_{50} values were calculated with the equation:

$$IC_{50} = \left(\frac{50\% - \text{low}\%}{\text{high}\% - \text{low}\%}\right)([\text{ribonuclease}]_{\text{high}} - [\text{ribonuclease}]_{\text{low}}) + [\text{ribonuclease}]_{\text{low}} \quad (4)$$

where low% and high% refer to inhibition by the two concentrations, $[\text{ribonuclease}]_{\text{low}}$ and $[\text{ribonuclease}]_{\text{high}}$, that bracket 50% inhibition.

Acknowledgements

We are grateful to B. D. Smith for providing a production system for hRI, and to Dr B. G. Miller, Dr M. T. Record Jr, J. E. Lee, S. M. Fuchs, and R. J. Johnson for contributive discussions. This work was supported by grant CA73808 (NIH). T.J.R. was supported by Biotechnology Training grant 08349 (NIH). E.L.K. was supported by a Pfizer Summer Undergraduate Research Fellowship, Wisconsin/Hilldale Undergraduate/Faculty Research Fellowship, University Bookstore Academic Excellence Award, and Trewartha Senior Thesis grant. The University of Wisconsin-Madison Biophysics Instrumentation Facility was established with grants BIR-9512577 (NSF) and RR13790 (NIH). The Keck–UWCCC Small Molecule Screening Facility was established with grants from the W. M. Keck Foundation and University of Wisconsin Comprehensive Cancer Center.

References

1. Raines, R. T. (1998). Ribonuclease A. *Chem. Rev.* **98**, 1045–1066.
2. D'Alessio, G. & Riordan, J. F. (1997). Editors of *Ribonucleases: Structures and Functions*, Academic Press, New York.
3. Leland, P. A. & Raines, R. T. (2001). Cancer chemotherapy–ribonucleases to the rescue. *Chem. Biol.* **8**, 405–413.
4. Matoušek, J. (2001). Ribonucleases and their antitumor activity. *Comp. Biochem. Physiol. C Toxicol. Pharmacol.* **129**, 175–191.
5. Makarov, A. A. & Ilinskaya, O. N. (2003). Cytotoxic ribonucleases: molecular weapons and their targets. *FEBS Letters*, **540**, 15–20.
6. Darzynkiewicz, Z., Carter, S. P., Mikulski, S. M., Ardelt, W. J. & Shogen, K. (1988). Cytostatic and cytotoxic effect of Pannon (P-30 protein), a novel anticancer agent. *Cell Tissue Kinet.* **21**, 169–182.
7. Mikulski, S. M., Ardelt, W., Shogen, K., Bernstein, E. H. & Menduke, H. (1990). Striking increase of survival of mice bearing M109 Madison carcinoma treated with a novel protein from amphibian embryos. *J. Natl Cancer Inst.* **82**, 151–153.
8. Saxena, S. K., Shogen, K. & Ardelt, W. (2003). ONCONASE® and its therapeutic potential. *Lab. Med.* **34**, 380–387.
9. Wu, Y., Mikulski, S. M., Ardelt, W., Rybak, S. M. & Youle, R. J. (1993). A cytotoxic ribonuclease. Study of the mechanism of onconase cytotoxicity. *J. Biol. Chem.* **268**, 10686–10693.
10. Mikulski, S. M., Costanzi, J. J., Vogelzang, N. J., McCachren, S., Taub, R. N., Chun, H. *et al*. (2002). Phase II trial of a single weekly intravenous dose of ranpirnase in patients with unresectable malignant mesothelioma. *J. Clin. Oncol.* **20**, 274–281.
11. Mikulski, S. M., Grossman, A. M., Carter, P. W., Shogen, K. & Costanzi, J. J. (1993). Phase I human clinical trial of ONCONASE (P-30 protein) administered intravenously on a weekly schedule in cancer patients with solid tumors. *Int. J. Oncol.* **3**, 57–64.
12. Boix, E., Wu, Y., Vasandani, V. M., Saxena, S. K., Ardelt, W., Ladner, J. & Youle, R. J. (1996). Role of the N terminus in RNase A homologues: differences in catalytic activity, ribonuclease inhibitor interaction and cytotoxicity. *J. Mol. Biol.* **257**, 992–1007.
13. Vasandani, V. M., Wu, Y. N., Mikulski, S. M., Youle, R. J. & Sung, C. (1996). Molecular determinants in the plasma clearance and tissue distribution of ribonucleases of the ribonuclease A superfamily. *Cancer Res.* **56**, 4180–4186.
14. Matoušek, J., Souček, J., Slavík, T., Tomanek, M., Lee, J. E. & Raines, R. T. (2003). Comprehensive comparison of the cytotoxic activities of onconase and bovine seminal ribonuclease. *Comp. Biochem. Physiol. C*, **136**, 343–356.
15. Ardelt, W., Mikulski, S. M. & Shogen, K. (1991). Amino acid sequence of an anti-tumor protein from *Rana pipiens* oocytes and early embryos. Homology to pancreatic ribonucleases. *J. Biol. Chem.* **266**, 245–251.
16. Hofsteenge, J. (1997). Ribonuclease inhibitor. In *Ribonucleases: Structures and Functions* (D'Alessio, G. & Riordan, J. F., eds), pp. 621–658, Academic Press, New York.
17. Shapiro, R. (2001). Cytoplasmic ribonuclease inhibitor. *Methods Enzymol.* **341**, 611–628.
18. Dickson, K. A., Haigis, M. C. & Raines, R. T. (2005). Ribonuclease inhibitor: structure and function. *Prog. Nucl. Acids Mol. Biol.* **80**, 349–374.
19. Kobe, B. & Deisenhofer, J. (1993). Crystal structure of porcine ribonuclease inhibitor, a protein with leucine-rich repeats. *Nature*, **366**, 751–756.
20. Kawanomoto, M., Motojima, K., Sasaki, M., Hattori, H. & Goto, S. (1992). cDNA cloning and sequence of rat ribonuclease inhibitor, and tissue distribution of mRNA. *Biochim. Biophys. Acta*, **1129**, 335–338.
21. Blazquez, M., Fominaya, J. M. & Hofsteenge, J. (1996). Oxidation of sulfhydryl groups of ribonuclease inhibitor in epithelial cells is sufficient for its intracellular degradation. *J. Biol. Chem.* **271**, 18638–18642.
22. Haigis, M. C., Kurten, E. L. & Raines, R. T. (2003). Ribonuclease inhibitor as an intracellular sentry. *Nucl. Acids Res.* **31**, 1024–1032.
23. Blackburn, P., Wilson, G. & Moore, S. (1977). Ribonuclease inhibitor from human placenta. Purification and properties. *J. Biol. Chem.* **252**, 5904–5910.
24. Kobe, B. & Deisenhofer, J. (1996). Mechanism of

ribonuclease inhibition by ribonuclease inhibitor protein based on the crystal structure of its complex with ribonuclease A. *J. Mol. Biol.* **264**, 1028–1043.
25. Vicentini, A. M., Kieffer, B., Matthies, R., Meyhack, B., Hemmings, B. A., Stone, S. R. & Hofsteenge, J. (1990). Protein chemical and kinetic characterization of recombinant porcine ribonuclease inhibitor expressed in *Saccharomyces cerevisiae*. *Biochemistry*, **29**, 8827–8834.
26. Murthy, B. S. & Sirdeshmukh, R. (1992). Sensitivity of monomeric and dimeric forms of bovine seminal ribonuclease to human placental ribonuclease inhibitor. *Biochem. J.* **281**, 343–348.
27. D'Alessio, G., Di Donato, A., Mazzarella, L. & Piccoli, R. (1997). Seminal ribonuclease: the importance of diversity. In *Ribonucleases: Structures and Functions* (D'Alessio, G. & Riordan, J. F., eds), pp. 383–423, Academic Press, New York.
28. Leland, P. A., Schultz, L. W., Kim, B. M. & Raines, R. T. (1998). Ribonuclease A variants with potent cytotoxic activity. *Proc. Natl Acad. Sci. USA*, **95**, 10407–10412.
29. Haigis, M. C., Kurten, E. L., Abel, R. L. & Raines, R. T. (2002). KFERQ sequence in ribonuclease A-mediated cytotoxicity. *J. Biol. Chem.* **277**, 11576–11581.
30. Mitchell, J. C., Kerr, R. & Ten Eyck, L. F. (2001). Rapid atomic density methods for molecular shape characterization. *J. Mol. Graph. Model.* **19**, 325–330, 388–390.
31. Crick, F. H. C. (1952). Is α-keratin a coiled coil? *Nature*, **170**, 882–883.
32. Mitchell, J. C., Shahbaz, S. & Ten Eyck, L. F. (2004). Interfaces in molecular docking. *Mol. Simul.* **30**, 97–106.
33. Kobe, B. & Deisenhofer, J. (1995). A structural basis of the interactions between leucine-rich repeats and protein ligands. *Nature*, **374**, 183–186.
34. Raines, R. T. (2004). Active site of ribonuclease A. In *Artificial Nucleases* (Zenkova, M. A., ed.), pp.19–32, Springer, Heidelberg.
35. Radzicka, A. & Wolfenden, R. (1988). Comparing the polarities of the amino acids: side-chain distribution coefficients between the vapor phase, cyclohexane, 1-octanol, and neutral aqueous solution. *Biochemistry*, **27**, 1664–1670.
36. Fuchs, S. M. & Raines, R. T. (2005). Polyarginine as a multifunctional fusion tag. *Protein Sci.* **14**, 1538–1544.
37. Rajamani, D., Thiel, S., Vajda, S. & Camacho, C. J. (2004). Anchor residues in protein–protein interactions. *Proc. Natl Acad. Sci. USA*, **101**, 11287–11292.
38. Neumann, U. & Hofsteenge, J. (1994). Interaction of semisynthetic variants of RNase A with ribonuclease inhibitor. *Protein Sci.* **3**, 248–256.
39. Kim, J. S., Souček, J., Matoušek, J. & Raines, R. T. (1995). Catalytic activity of bovine seminal ribonuclease is essential for its immunosuppressive and other biological activities. *Biochem. J.* **308**, 547–550.
40. Lee, J. E. & Raines, R. T. (2003). Contribution of active-site residues to the function of onconase, a ribonuclease with antitumoral activity. *Biochemistry*, **42**, 11443–11450.
41. Boix, E., Nogues, M. V., Schein, C. H., Benner, S. A. & Cuchillo, C. M. (1994). Reverse transphosphorylation by ribonuclease A needs an intact p2-binding site. Point mutations at Lys-7 and Arg-10 alter the catalytic properties of the enzyme. *J. Biol. Chem.* **269**, 2529–2534.
42. Nogues, M. V., Vilanova, M. & Cuchillo, C. M. (1995). Bovine pancreatic ribonuclease A as a model of an enzyme with multiple substrate binding sites. *Biochim. Biophys. Acta*, **1253**, 16–24.
43. Fisher, B. M., Ha, J. H. & Raines, R. T. (1998). Coulombic forces in protein-RNA interactions: binding and cleavage by ribonuclease A and variants at Lys7, Arg10, and Lys66. *Biochemistry*, **37**, 12121–12132.
44. Kobe, B. & Deisenhofer, J. (1995). Proteins with leucine-rich repeats. *Curr. Opin. Struct. Biol.* **5**, 409–416.
45. Chen, C. Z. & Shapiro, R. (1999). Superadditive and subadditive effects of "hot spot" mutations within the interfaces of placental ribonuclease inhibitor with angiogenin and ribonuclease A. *Biochemistry*, **38**, 9273–9285.
46. Klink, T. A. & Raines, R. T. (2000). Conformational stability is a determinant of ribonuclease A cytotoxicity. *J. Biol. Chem.* **275**, 17463–17467.
47. Bretscher, L. E., Abel, R. L. & Raines, R. T. (2000). A ribonuclease A variant with low catalytic activity but high cytotoxicity. *J. Biol. Chem.* **275**, 9893–9896.
48. Gaur, D., Swaminathan, S. & Batra, J. K. (2001). Interaction of human pancreatic ribonuclease with human ribonuclease inhibitor. Generation of inhibitor-resistant cytotoxic variants. *J. Biol. Chem.* **276**, 24978–24984.
49. Youle, R. J. & D'Alessio, G. (1997). Antitumor RNases. In *Ribonucleases: Structures and Functions* D'Alessio, G. & Riordan, J. F., eds), pp. 491–514, Academic Press, New York.
50. Dickson, K. A., Dahlberg, C. L. & Raines, R. T. (2003). Compensating effects on the cytotoxicity of ribonuclease A variants. *Arch. Biochem. Biophys.* **415**, 172–177.
51. Lo Conte, L., Chothia, C. & Janin, J. (1999). The atomic structure of protein–protein recognition sites. *J. Mol. Biol.* **285**, 2177–2198.
52. Janin, J. (1995). Elusive affinities. *Proteins: Struct. Funct. Genet.* **21**, 30–39.
53. Miller, S., Janin, J., Lesk, A. M. & Chothia, C. (1987). Interior and surface of monomeric proteins. *J. Mol. Biol.* **196**, 641–656.
54. Ui, N. (1971). Isolectric points and conformation of proteins. I. Effect of urea on the behavior of some proteins in isoelectric focusing. *Biochim. Biophys. Acta*, **229**, 567–581.
55. Lawrence, M. C. & Colman, P. M. (1993). Shape complementarity at protein/protein interfaces. *J. Mol. Biol.* **234**, 946–950.
56. Messmore, J. M., Fuchs, D. N. & Raines, R. T. (1995). Ribonuclease A: revealing structure–function relationships with semisynthesis. *J. Am. Chem. Soc.* **117**, 8057–8060.
57. Lee, F. S., Shapiro, R. & Vallee, B. L. (1989). Tight-binding inhibition of angiogenin and ribonuclease A by placental ribonuclease inhibitor. *Biochemistry*, **28**, 225–230.
58. Chen, C. Z. & Shapiro, R. (1997). Site-specific mutagenesis reveals differences in the structural bases for tight binding of RNase inhibitor to angiogenin and RNase A. *Proc. Natl Acad. Sci. USA*, **94**, 1761–1766.
59. Nadano, D., Yasuda, T., Takeshita, H., Uchide, K. & Kishi, K. (1994). Purification and characterization of human brain ribonuclease inhibitor. *Arch. Biochem. Biophys.* **312**, 421–428.
60. Raines, R. T. (1999). Ribonuclease A: from model system to cancer chemotherapeutic. In *Enzymatic Mechanisms* (Frey, P. A., & Northrop, D. B., eds), pp. 235–249, IOS Press, Washington, DC.
61. Futami, J., Nukui, E., Maeda, T., Kosaka, M., Tada, H., Seno, M. & Yamada, H. (2002). Optimum modification for the highest cytotoxicity of cationized ribonuclease. *J. Biochem. (Tokyo)*, **132**, 223–228.

62. Futami, J., Maeda, T., Kitazoe, M., Nukui, E., Tada, H., Seno, M. *et al*. (2001). Preparation of potent cytotoxic ribonucleases by cationization: enhanced cellular uptake and decreased interaction with ribonuclease inhibitor by chemical modification of carboxyl groups. *Biochemistry*, **40**, 7518–7524.
63. Ilinskaya, O. N., Dreyer, F., Mitkevich, V. A., Shaw, K. L., Pace, C. N. & Makarov, A. A. (2002). Changing the net charge from negative to positive makes ribonuclease Sa cytotoxic. *Protein Sci.* **11**, 2522–2525.
64. Kuhn, L. A., Siani, M. A., Pique, M. E., Fisher, C. L., Getzoff, E. D. & Tainer, J. A. (1992). The interdependence of protein surface topography and bound water molecules revealed by surface accessibility and fractal density measures. *J. Mol. Biol.* **228**, 13–22.
65. Abel, R. L., Haigis, M. C., Park, C. & Raines, R. T. (2002). Fluorescence assay for the binding of ribonuclease A to the ribonuclease inhibitor protein. *Anal. Biochem.* **306**, 100–107.
66. Kunkel, T. A., Roberts, J. D. & Zakour, R. A. (1987). Rapid and efficient site-specific mutagenesis without phenotypic selection. *Methods Enzymol.* **154**, 367–382.
67. delCardayré, S. B., Ribo, M., Yokel, E. M., Quirk, D. J., Rutter, W. J. & Raines, R. T. (1995). Engineering ribonuclease A: production, purification and characterization of wild-type enzyme and mutants at Gln11. *Protein Eng.* **8**, 261–273.
68. Sela, M., Anfinsen, C. B. & Harrington, W. F. (1957). The correlation of ribonuclease activity with specific aspects of tertiary structure. *Biochim. Biophys. Acta*, **26**, 502–512.
69. Klink, T. A., Vicentini, A. M., Hofsteenge, J. & Raines, R. T. (2001). High-level soluble production and characterization of porcine ribonuclease inhibitor. *Protein Expr. Purif.* **22**, 174–179.
70. Eberhardt, E. S., Wittmayer, P. K., Templer, B. M. & Raines, R. T. (1996). Contribution of a tyrosine side chain to ribonuclease A catalysis and stability. *Protein Sci.* **5**, 1697–1703.
71. Kelemen, B. R., Klink, T. A., Behlke, M. A., Eubanks, S. R., Leland, P. A. & Raines, R. T. (1999). Hypersensitive substrate for ribonucleases. *Nucl. Acids Res.* **27**, 3696–3701.
72. Smith, B. D., Soellner, M. B. & Raines, R. T. (2003). Potent inhibition of ribonuclease A by oligo(vinylsulfonic acid). *J. Biol. Chem.* **278**, 20934–20938.
73. Zhang, J. H., Chung, T. D. & Oldenburg, K. R. (1999). A simple statistical parameter for use in evaluation and validation of high throughput screening assays. *J. Biomol. Screen.* **4**, 67–73.

Edited by B. Honig

(Received 10 May 2005; received in revised form 6 August 2005; accepted 8 August 2005)
Available online 24 August 2005